RSC Advances

PAPER

View Article Online
View Journal | View Issue

Cite this: *RSC Adv.*, 2022, **12**, 9058

Application of novel metal–organic framework [Zr-UiO-66-PDC-SO_3H]$FeCl_4$ in the synthesis of dihydrobenzo[*g*]pyrimido[4,5-*b*]quinoline derivatives†

Fatemeh Jalili, Mahmoud Zarei, * Mohammad Ali Zolfigol * and Ardeshir Khazaei*

Received 29th November 2021
Accepted 8th March 2022

DOI: 10.1039/d1ra08710j

rsc.li/rsc-advances

In the current paper, we produce a new metal–organic framework (MOF) based on Zr metal, [Zr-UiO-66-PDC-SO_3H]$FeCl_4$, *via* an anion exchange method, which is fully characterized by FT-IR, SEM with elemental mapping and EDX, FE-SEM and TEM. Furthermore, the use of [Zr-UiO-66-PDC-SO_3H]$FeCl_4$ as a porous catalyst was examined for the one-pot synthesis of novel dihydrobenzo[*g*]pyrimido[4,5-*b*]quinoline derivatives by reaction of 6-amino-1,3-dimethylpyrimidine-2,4(1*H*,3*H*)-dione, 2-hydroxynaphthalene-1,4-dione and various aldehydes at 100 °C with good to excellent yields.

Introduction

Nowadays, porous materials such as metal–organic frameworks (MOFs) are of great interest to scientists.[1,2] These crystalline materials comprise metal and organic compounds as the nucleus and ligands, respectively. MOFs are multifunctional materials that have been used as adsorbents for the storage and separation of gas, drug delivery, catalyst, proton conductivity and heavy metal adsorbents.[3–9] Post- modification and synthesis of MOFs with acid functional groups and metal have been reported for the transportation of organic compounds, oxidation, and synthesis of biological compounds.[10] Lillerud *et al.* reported the first MOFs based on Zr, such as Zr-UiO-66-PDC.[11] Considering this, the new class of porous catalyst with sulfonic and phosphorus acid tag-MOFs have been applied in the preparation of pyrimido[4,5-*b*]quinolones and dicyanomethylene pyridine derivatives – *N*-amino-2-pyridone and pyrano [2,3-*c*] pyrazole derivatives.[12–15]

Anion exchange is an architectonic method for the preparation of ionic liquids (ILs) and/or molten salts (MSs) with several opposing ions that cannot be synthesized directly. Our research group has introduced MSs with N–S bonds as a new category of catalyst and reagent based on organic materials.[16–24] Now, we combine the porous materials MOF Zr-UiO-66-PDC with $ClSO_3H$, to prepare [Zr-UiO-66-PDC-SO_3H]Cl as a novel porous catalyst for ILs.

Recently, *N*-heterocyclic scaffold compounds have been considered as candidates for the design and discovery of new biologically active compounds. It is very important to supply new and easy methods for the preparation of target compounds with unique features. In this regard, 1,4-dihydropyridine structures containing uracil and henna (2-hydroxynaphthalene-1,4-dione) moieties are suitable candidates for biological and pharmacological purposes.[25–29] These molecules have been used as drugs in furnidipine and alogliptin (Fig. 1).[30,31] Also, scaffolds with uracil moieties have been reported as having antitumour,[32] cardiotonic,[33] hepatoprotactive,[34] antihypertensive,[35] antibronchitic[36] and antifungal activity.[37] Therefore, the appearance of novel and simple organic synthetic approaches for the efficient preparation of this type of heterocycle is an interesting challenge. Since scaffolds with uracil and henna moieties are of biological interest,[38,39] we synthesize 1,4-dihydropyridine with uracil and henna moieties.

In continuation of our investigation on the development and preparation of MOFs with sulfonic acid tags and organic molecules with henna moieties,[40] in this paper, we prepare [Zr-UiO-66-PDC-SO_3H]$FeCl_4$ as an efficient and novel porous catalyst for new dihydrobenzo[*g*]pyrimido[4,5-*b*]quinoline derivatives by condensation reaction of 2-hydroxynaphthalene-1,4-dione, 6-amino-1,3-dimethylpyrimidine-2,4(1*H*,3*H*)-dione and various aldehydes (mono and bis) under solvent free conditions at 100 °C (Fig. 2).

Experimental

Preparation of [Zr-UiO-66-PDC-SO_3H]$FeCl_4$

Initially, our MOFs [Zr-UiO-66-PDC] were synthesized according to a previously reported methodology.[41] In a round-bottomed flask, 50 mL, a mixture of $ClSO_3H$ (2 mmol, 0.134 mL) and [Zr-UiO-66-PDC] (0.564 g) in dry CH_2Cl_2 (30 mL) at 0 °C was stirred for 2 hours. After this, a white precipitate appeared which was separated (by centrifugation) and dried under

Department of Organic Chemistry, Faculty of Chemistry, Bu-Ali-Sina University, 6517838965, Hamedan, Iran. E-mail: Mahmoud8103@yahoo.com; zolfi@basu.ac.ir; mzolfigol@yahoo.com; Khazaei_1326@yahoo.com

† Electronic supplementary information (ESI) available. See DOI: 10.1039/d1ra08710j

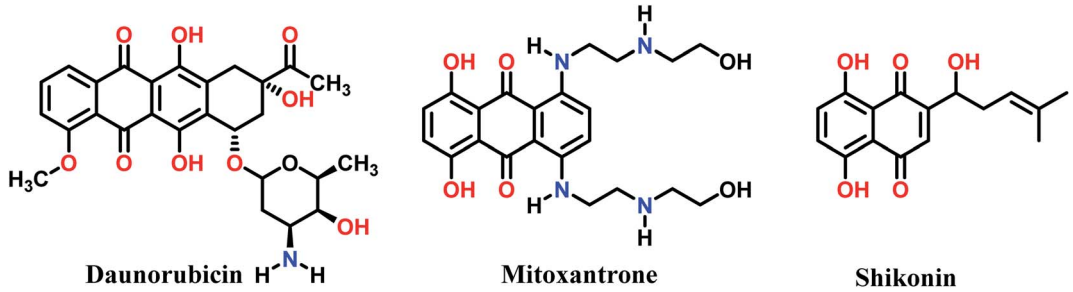

Fig. 1 Biological compounds containing uracil, henna and dihydropyridine moieties in their structures.

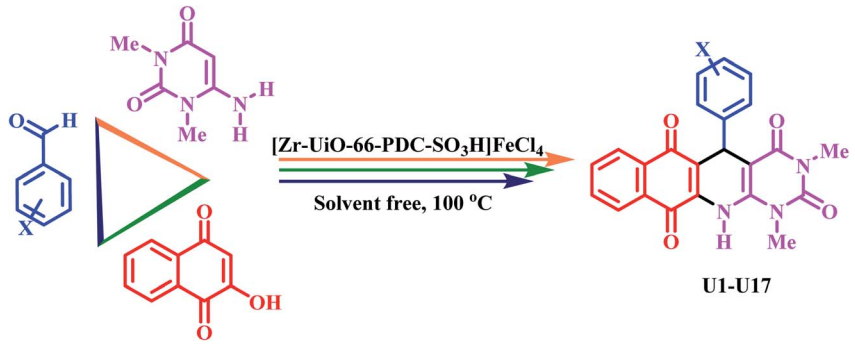

Fig. 2 Preparation of dihydrobenzo[*g*]pyrimido[4,5-*b*]quinoline using [Zr-UiO-66-PDC-SO_3H]$FeCl_4$.

vacuum. Then, according to the anion exchange method, a mixture of [Zr-UiO-66-PDC-SO_3H]Cl (2 g) and $FeCl_3$ (5 mmol, 0.81 g) was stirred in a mortar at 50 °C for 2 hours. After completion of the reaction, the reaction mixture was cooled down to room temperature. Finally, acetone was used to purify the [Zr-UiO-66-PDC-SO_3H]$FeCl_4$ *via* trituration (Fig. 3).

General procedure for the synthesis of dihydrobenzo[*g*]pyrimido[4,5-*b*]quinoline derivatives using [Zr-UiO-66-PDC-SO_3H]$FeCl_4$

In a 15 mL round-bottomed flask, a mixture of 2-hydroxynaphthalen-1,4-dione (henna, 1 mmol, 0.174 g), 6-amino-1,3-dimethylpyrimidine-2,4(1*H*,3*H*)-dione (1 mmol, 0.155 g) and aldehyde (1 mmol) in the presence of 10 mg of [Zr-UiO-66-PDC-SO_3H]$FeCl_4$ was stirred at 100 °C under solvent-free conditions. After the completion of the reactions which were monitored by the TLC technique (2 : 3 *n*-hexane : ethyl acetate). The described catalyst was separated from the reaction mixture by centrifugation (1000 rpm) after adding 10 mL of EtOH as solvent. Finally, after the evaporation of the solvent at room temperature, pure product was obtained by washing with hot ethanol and water (Fig. 2).

Spectra data

1,3-Dimethyl-5-(*p*-tolyl)-5,12-dihydrobenzo[*g*]pyrimido[4,5-*b*]quinolone 2,4,6,11(1*H*,3*H*)-tetraone (U1). Red solid; Mp: 280 °C dec.; FT-IR (KBr) υ (cm^{-1}) = 3401, 3245, 1702, 1575, 1510. ^{1}H NMR (400 MHz, DMSO-d_6) δ 7.89 (d, J = 7.5 Hz, 1H), 7.80 (d, J = 7.1 Hz, 1H), 7.69 (t, J = 8.0 Hz, 1H), 7.62 (s, 1H), 7.57 (t, J = 7.6 Hz, 1H), 6.95 (s, 4H), 6.30 (s, 1H), 3.31 (s, 3H), 3.21 (s, 3H), 2.26 (s, 3H). ^{13}C NMR (101 MHz, DMSO) δ 180.3, 162.3, 150.6, 135.4, 133.4, 132.5, 131.2, 130.4, 127.9, 126.6, 125.7, 125.4, 125.2, 124.7, 87.0, 34.4, 29.6, 28.1, 20.5. MS: m/z (%) = 413.2.

1,3-Dimethyl-5-(4-nitrophenyl)-5,12-dihydrobenzo[*g*]pyrimido[4,5-*b*]quinoline 2,4,6,11(1*H*,3*H*)-tetraone (U2). Red solid; Mp: >300 °C; FT-IR (KBr) υ (cm^{-1}) = 3396, 3230, 1694, 1656, 1605, 1576, 1342. ^{1}H NMR (400 MHz, DMSO-d_6) δ 7.86 (d, J = 7.6 Hz, 1H), 7.77 (d, J = 6.4 Hz, 1H), 7.66 (t, J = 5.6 Hz, 1H), 7.54 (s, 2H), 7.16 (d, J = 7.4 Hz, 2H), 7.03 (d, J = 6.9 Hz, 2H), 6.27 (s, 1H), 3.27 (s, 3H), 3.18 (s, 3H). ^{13}C NMR (101 MHz, DMSO-d_6) δ 180.0, 150.7, 135.4, 133.4, 131.3, 130.3, 128.6, 128.2, 127.6, 127.1, 125.4, 124.7, 119.1, 86.4, 34.5, 29.5, 28.1. MS: m/z (%) = 444.1.

5-(4-Chlorophenyl)-1,3-dimethyl-5,12-dihydrobenzo[*g*]pyrimido[4,5-*b*]quinoline-2,4,6,11(1*H*,3*H*)-tetraone (U3). Red solid; Mp: >300 °C; FT-IR (KBr) υ (cm^{-1}) = 3456, 3336, 1693, 1596, 1508. ^{1}H NMR (400 MHz, DMSO-d_6) δ 8.00 (d, J = 8.7 Hz, 2H), 7.86 (d, J = 7.5 Hz, 1H), 7.77 (d, J = 7.3 Hz, 1H), 7.66 (t, J = 7.2 Hz, 1H), 7.53 (t, J = 7.3 Hz, 1H), 7.47 (s, 1H), 7.26 (d, J = 8.4 Hz, 2H), 6.39 (s, 1H), 3.26 (s, 3H), 3.17 (s, 3H). ^{13}C NMR (101 MHz, DMSO) δ 185.8, 179.6, 161.7, 154.3, 152.6, 150.8, 144.4, 135.4, 133.4, 131.3, 130.3, 127.9, 127.8, 125.4, 124.7, 122.6, 118.6, 85.8, 35.8, 29.5, 27.9. MS: m/z (%) = 433.1[M], 435.2 [M + 2].

5-(3,4-Difluorophenyl)-1,3-dimethyl-5,12-dihydrobenzo[*g*]pyrimido[4,5-*b*]quinoline-2,4,6,11(1*H*,3*H*)-tetraone (U4). Red solid; Mp:>300 °C; FT-IR (KBr) υ (cm^{-1}) = 3392, 3061, 1691,1669, 1591, 1510. ^{1}H NMR (400 MHz, DMSO-d_6) δ 7.88–7.85 (m, 1H), 7.77–7.74 (m, 1H), 7.68–7.64 (m, 1H), 7.54–7.50 (m, 1H), 7.44 (s, 1H), 7.16–7.09 (m, 1H), 6.90 (d J = 9.1 Hz, 1H), 6.83–6.77 (m, 1H), 6.27 (s, 1H), 3.25 (s, 3H), 3.16 (s, 3H). ^{13}C

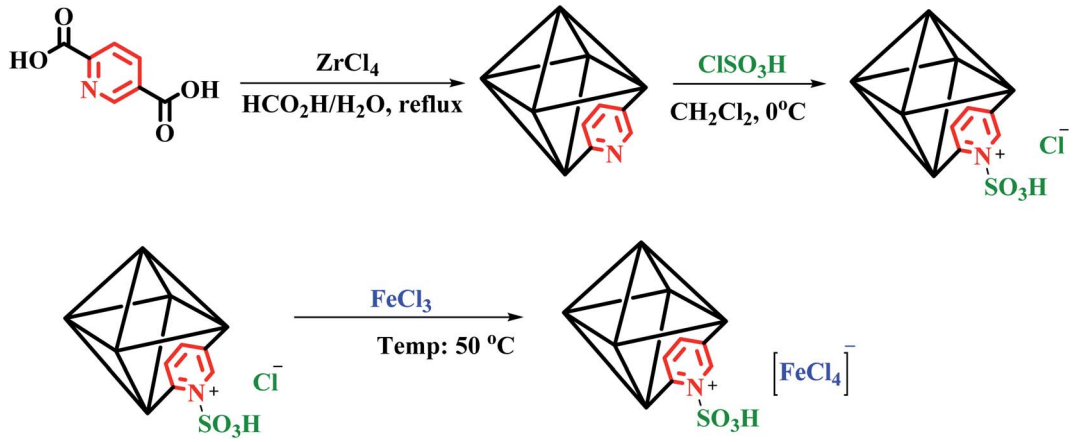

Fig. 3 Preparation of [Zr-UiO-66-PDC-SO_3H]$FeCl_4$.

NMR (100 MHz, DMSO) δ 163.9, 154.4, 152.1, 147.9, 140.9, 133.8, 132.5, 129.5, 124.0, 123.3, 121.2, 120.8, 116.9, 114.3, 93.4, 37.2, 30.4, 29.0. MS: m/z (%) = 435.2.

1,3-Dimethyl-5-(4-(trifluoromethyl)phenyl)-5,12-dihydrobenzo[*g*]pyrimido[4,5-*b*]quinoline-2,4,6,11(1*H*,3*H*)-tetraone (U5). Red solid; Mp: 290 °C dec.; FT-IR (KBr) υ (cm^{-1}) = 3403, 3247, 1702, 1603, 1575, 1511. ^{1}H NMR (400 MHz, DMSO-d_6) δ 7.96 (d, J = 7.5 Hz, 1H), 7.87 (d, J = 7.4 Hz, 1H), 7.76 (t, J = 7.3 Hz, 1H), 7.66–7.60 (m, 2H), 7.56 (d, J = 8.1 Hz, 2H), 7.32 (d, J = 7.9 Hz, 2H), 6.45 (s, 1H), 3.36 (s, 3H), 3.27 (s, 3H). ^{13}C NMR (101 MHz, DMSO-d_6) δ 185.6, 162.0, 152.9, 150.7, 135.4, 133.4, 131.3, 130.4, 127.3, 126.2, 125.4, 124.7, 124.2, 118.9, 86.1, 35.2, 29.6, 28.1. MS: m/z (%) = 467.1.

5-(3,5-Difluorophenyl)-1,3-dimethyl-5,12-dihydrobenzo[*g*]pyrimido[4,5-*b*]quinoline-2,4,6,11(1*H*,3*H*)-tetraone (U6). Red solid; Mp: >300 °C; FT-IR (KBr) υ (cm^{-1}) = 3393, 3238, 1691, 1659, 1594, 1509. ^{1}H NMR (400 MHz, DMSO-d_6) δ 8.00 (d, J = 7.4 Hz, 1H), 7.89 (d, J = 7.1 Hz, 1H), 7.81–7.77 (m, 1H), 7.66 (t, J = 7.4 Hz, 1H), 6.94 (s, 1H), 6.77 (s, 1H), 6.75 (s, 1H), 6.41 (s, 1H), 3.38 (s, 3H), 3.29 (s, 3H). ^{13}C NMR (100 MHz, DMSO) δ 183.5, 150.7, 133.8, 133.2, 131.9, 130.9, 128.7, 128.4, 128.1, 125.7, 125.1, 123.3, 121.8, 117.7, 116.4, 115.8, 53.5, 32.5, 29.6, 28.0. MS: m/z (%) = 436.2.

5-(3-Hydroxyphenyl)-1,3-dimethyl-5,12-dihydrobenzo[*g*]pyrimido[4,5-*b*]quinoline-2,4,6,11(1*H*,3*H*)-tetraone (U7). Red solid; Mp:280 °C dec.; FT-IR (KBr) υ (cm^{-1}) = 3397, 3250, 1674, 1609, 1578, 1512. ^{1}H NMR (400 MHz, DMSO-d_6) δ 8.83 (s, 1H), 7.92 (d, J = 7.6 Hz, 1H), 7.81 (d, J = 7.2 Hz, 1H), 7.71 (t, J = 7.2 Hz, 1H), 7.60 (s, 1H), 7.57 (d, J = 7.3 Hz, 1H), 6.95 (t, J = 7.7 Hz, 1H), 6.53 (d, J = 7.4 Hz, 2H), 6.45 (d, J = 7.8 Hz, 1H), 6.29 (s, 1H), 3.33 (s, 3H), 3.23 (s, 3H). ^{13}C NMR (101 MHz, DMSO-d_6) δ 182.1, 156.7, 135.7, 133.4, 131.3, 130.2, 127.9, 125.4, 124.5, 119.6, 117.7, 113.7, 110.8, 87.0, 34.8, 29.5, 28.0. MS: m/z (%) = 415.1.

1,3-Dimethyl-5-phenyl-5,12-dihydrobenzo[*g*]pyrimido[4,5-*b*]quinoline-2,4,6,11(1*H*,3*H*)-tetraone (U8). Red solid; Mp: 255–256 °C; FT-IR (KBr) υ (cm^{-1}) = 3407, 3244, 1699, 1605, 1578, 1509. ^{1}H NMR (400 MHz, DMSO-d_6) δ 13.21 (s, 1H), 8.03 (d, J = 7.4 Hz, 1H), 8.00 (d, J = 8.5 Hz, 1H), 7.87–7.80 (m, 2H), 7.22 (dt, J = 16.9, 5.6 Hz, 5H), 5.86 (s, 1H), 3.38 (s, 3H), 3.15 (s, 3H). ^{13}C NMR (101 MHz, DMSO-d_6) δ 181.1, 163.6, 154.3, 150.1, 138.4, 134.3, 133.9, 133.5, 132.0, 131.7, 130.5, 128.0, 127.7, 126.7, 126.0, 125.7, 125.1, 124.8, 123.4, 85.6, 34.7, 30.4, 28.2. MS: m/z (%) = 399.2.

5-(2-Methoxyphenyl)-1,3-dimethyl-5,12-dihydrobenzo[*g*]pyrimido[4,5-*b*]quinoline-2,4,6,11(1*H*,3*H*)-tetraone (U9). Red solid; Mp: 288 °C dec.; FT-IR (KBr) υ(cm^{-1}) = 3442, 3355, 1696, 1633, 1657, 1504. ^{1}H NMR (400 MHz, DMSO-d_6) δ 9.02 (s, 1H), 8.06 (s, 1H), 7.99–7.71 (m, 3H), 7.25 (d, J = 100.1 Hz, 2H), 6.96–6.75 (m, 2H), 5.31 (s, 1H), 3.70 (s, 3H), 3.61 (s, 3H), 3.09 (s, 3H). ^{13}C NMR (101 MHz, DMSO-d_6) δ 181.8, 160.4, 150.6, 139.4, 135.0, 133.5, 131.6, 128.1, 125.9, 125.8, 125.8, 122.5, 119.7, 111.8, 88.3, 55.4, 33.8, 29.7, 27.6. MS: m/z (%) = 429.2.

5-(2,4-Dichlorophenyl)-1,3-dimethyl-5,12-dihydrobenzo[*g*]pyrimido[4,5-*b*]quinoline-2,4,6,11(1*H*,3*H*)-tetraone (U10). Red solid; Mp: >300 °C; FT-IR (KBr) υ (cm^{-1}) = 3456, 3336, 1693, 1596, 1508. ^{1}H NMR (400 MHz, DMSO-d_6) δ 7.96 (s, 2H), 7.89 (s, 1H), 7.77 (s, 1H), 7.69 (s, 1H), 7.41 (s, 1H), 7.35 (s, 1H), 7.27 (s, 1H), 6.51 (s, 1H), 2.90 (s, 3H), 2.74 (s, 3H).^{13}C NMR (101 MHz, DMSO-d_6) δ 177.9, 176.9, 158.9, 158.6, 156.4, 153.0, 151.8, 150.5, 150.4, 136.6, 136.6, 135.4, 134.9, 132.6, 132.4, 132.3, 132.1, 131.9, 128.8, 128.2, 127.8, 127.7, 127.2, 127.0, 126.8, 121.3, 104.2, 79.3, 31.3, 30.0, 28.0. MS: m/z (%) = 466.8 [M], 469 [M + 2].

5-(4-Methoxyphenyl)-1,3-dimethyl-5,12-dihydrobenzo[*g*]pyrimido[4,5-*b*]quinoline-2,4,6,11(1*H*,3*H*)-tetraone (U11). Red solid; Mp: 232–234 °C; FT-IR (KBr) υ (cm^{-1}) = 3398, 3238, 1702, 1607, 1580, 1511.^{1}H NMR (400 MHz, DMSO-d_6) δ 8.04–7.99 (m, 1H), 7.98 (d, J = 7.3 Hz, 1H), 7.86–7.78 (m, 2H), 7.20 (s, 1H), 7.09 (d, J = 8.3 Hz, 2H), 6.79 (d, J = 8.7 Hz, 2H), 5.80 (s, -1H), 3.71 (s, 3H), 3.36 (s, 3H), 3.14 (s, 3H). ^{13}C NMR (101 MHz, DMSO-d_6) δ 163.4, 157.2, 154.2, 150.2, 134.3, 133.8, 133.3, 130.5, 127.7, 126.0, 125.6, 113.4, 85.9, 54.9, 34.0, 30.3, 28.1. MS: m/z (%) = 429.1.

5-(4-(Dimethylamino)phenyl)-1,3-dimethyl-5,12-dihydrobenzo[*g*]pyrimido[4,5-*b*]quinoline-2,4,6,11(1*H*,3*H*)-tetraone (U12). Red solid; Mp: 230 °C dec.; FT-IR (KBr) υ (cm^{-1}) = 3402, 3357, 1671, 1597, 1574, 1515. ^{1}H NMR (400 MHz, DMSO-d_6) δ 7.92 (d, J = 7.7 Hz, 1H), 7.82 (d, J = 7.3 Hz, 1H), 7.75–7.68 (m, 1H), 7.61–7.56 (m, 1H), 6.90 (d, J = 8.4 Hz, 1H), 6.86 (s, 2H), 6.62

(d, J = 8.5 Hz, 1H), 4.77 (s, 1H), 3.31 (s, 3H), 3.24 (s, 3H), 3.14 (s, 3H), 2.87 (s, 3H). ^{13}C NMR (101 MHz, DMSO-d_6) δ 185.4, 180.6, 163.1, 158.0, 153.9, 149.7, 145.1, 135.1, 133.9, 133.0, 131.2, 130.1, 126.1, 125.5, 125.2, 123.2, 85.2, 40.6, 34.0, 30.0, 27.7. MS: m/z (%) = 441.2.

5-(4-Isopropylphenyl)-1,3-dimethyl-5,12-dihydrobenzo[*g*]pyrimido[4,5-*b*]quinoline-2,4,6,11(1*H*,3*H*)-tetraone (U13). Red solid; Mp: >300 °C; FT-IR (KBr) υ (cm^{-1}) = 3408, 3130, 2925, 1668, 1590, 1511. ^{1}H NMR (400 MHz, DMSO-d_6) δ 7.85 (d, J = 7.5 Hz, 1H), 7.73 (d, J = 7.6 Hz, 1H), 7.64 (t, J = 7.4 Hz, 1H), 7.53–7.47 (m, 2H), 6.96 (d, J = 8.1 Hz, 2H), 6.90 (d, J = 7.9 Hz, 2H), 6.24 (s, 1H), 3.25 (s, 3H), 3.15 (s, 3H), 2.82–2.74 (m, 1H), 1.17 (d, J = 6.8 Hz, 6H). ^{13}C NMR (101 MHz, DMSO-d_6) δ 185.9, 181.1, 163.6, 158.5, 154.4, 150.1, 145.5, 135.6, 134.3, 133.5, 131.7, 130.6, 126.6, 126.1, 126.0, 125.7, 123.7, 85.6, 34.4, 32.9, 30.4, 28.2, 24.0, 23.9. MS: m/z (%) = 441.2.

5-(4-Hydroxyphenyl)-1,3-dimethyl-5,12-dihydrobenzo[*g*]pyrimido[4,5-*b*]quinoline-2,4,6,11(1*H*,3*H*)-tetraone (U14). Red solid; Mp: 220 °C dec.; FT-IR (KBr) υ (cm^{-1}) = 3393, 3229, 1671, 1654, 1509. ^{1}H NMR (400 MHz, DMSO-d_6) δ 8.49 (s, 1H), 7.86 (d, J = 7.7 Hz, 1H), 7.75 (d, J = 7.6 Hz, 1H), 7.65 (t, J = 7.5 Hz, 2H), 7.52 (d, J = 7.5 Hz, 2H), 7.43 (s, 1H), 7.17–7.07 (m, 2H), 6.90 (d, J = 7.8 Hz, 2H), 6.26 (s, 1H), 3.24 (s, 3H), 3.16 (s, 3H). ^{13}C NMR (101 MHz, DMSO-d_6) δ 180.0, 150.7, 142.9, 135.4, 133.4, 131.3, 130.3, 128.6, 128.2, 127.1, 125.4, 124.7, 86.4, 34.5, 29.5, 28.1. MS: m/z (%) = 415.2.

1,3-Dimethyl-5-(3-nitrophenyl)-5,12-dihydrobenzo[*g*]pyrimido[4,5-*b*]quinoline-2,4,6,11(1*H*,3*H*)-tetraone (U15). Red solid; Mp: 300 °C dec.; FT-IR (KBr) υ (cm^{-1}) = 3334, 3508, 1717, 1682, 1562, 1529. ^{1}H NMR (400 MHz, DMSO-d_6) δ 7.90 (d, J = 7.9 Hz, 1H), 7.87 (d, J = 8.2 Hz, 1H), 7.78 (s, 1H), 7.67 (t, J = 7.1 Hz, 1H), 7.56–7.51 (m, 1H), 7.49–7.39 (m, 3H), 6.39 (s, 1H), 3.27 (s, 3H), 3.17 (s, 3H). ^{13}C NMR (101 MHz, DMSO-d_6) δ 185.8, 179.8, 161.7, 152.7, 150.8, 147.6, 147.3, 135.4, 133.8, 133.4, 131.4, 130.3, 128.7, 125.4, 124.7, 121.2, 119.1, 118.4, 85.8, 35.2, 29.5, 28.0. MS: m/z (%) = 444.1.

5,5'-(1,3-Phenylene)bis(1,3-dimethyl-5,12-dihydrobenzo[*g*]pyrimido[4,5-*b*]quinoline-2,4,6,11(1*H*,3*H*)-tetraone) (U16). Red solid; Mp: >300 °C; FT-IR (KBr) υ (cm^{-1}) = 3396, 3200, 1682, 1608, 1579, 1508.^{1}H NMR (400 MHz, DMSO-d_6) δ 8.00 (d, J = 7.9 Hz, 2H), 7.97 (d, J = 8.2 Hz, 2H), 7.88 (s, 2H), 7.77 (t, J = 7.1 Hz, 2H), 7.66–7.61 (m, 2H), 7.57 (d, J = 7.2 Hz, 2H), 7.55–7.50 (m, 2H), 6.49 (s, 2H), 3.37 (s, 6H), 3.27 (s, 6H). ^{13}C NMR (101 MHz, DMSO-d_6) δ 193.8, 161.7, 152.6, 150.9, 145.8, 135.8, 135.6, 133.4, 131.4, 130.2, 128.1, 127.9, 125.6, 125.4, 124.6, 118.9, 86.2, 35.0, 29.5, 27.9. MS: m/z (%) = 718.1.

5,5'-(1,4-Phenylene)bis(1,3-dimethyl-5,12-dihydrobenzo[*g*]pyrimido[4,5-*b*]quinoline-2,4,6,11(1*H*,3*H*)-tetraone) (U17). Red solid; Mp: 289 °C dec.; FT-IR (KBr) υ (cm^{-1}) = 3396, 3200, 1682, 1608, 1579, 1508. ^{1}H NMR (400 MHz, DMSO-d_6) δ 1H NMR (400 MHz, DMSO-d6) δ 9.97 (s, 2H), 7.93 (d, J = 7.5 Hz, 2H), 7.85 (d, J = 7.4 Hz, 2H), 7.74 (d, J = 7.8 Hz, 4H), 7.31 (d, J = 7.7 Hz, 4H), 6.45 (s, 2H), 3.35 (s, 6H), 3.25 (s, 6H). ^{13}C NMR (101 MHz, DMSO-d_6) δ 185.8, 153.7, 144.6, 142.9, 137.8, 127.7, 127.5, 125.3, 123.4, 122.1, 120.1, 119.9, 117.5, 117.3, 116.5, 110.8, 78.2, 26.9, 21.5, 19.9. MS: m/z (%) = 718.1.

Results and discussion

To improve the catalytic application of MOFs, we have designed and synthesized [Zr-UiO-66-PDC-SO_3H]Cl. Post-functionalization of [Zr-UiO-66-PDC] occurred by preparing [Zr-UiO-66-PDC-SO_3H]$FeCl_4$ using $FeCl_3$ in a mortar at room temperature (Fig. 3). [Zr-UiO-66-PDC-SO_3H]$FeCl_4$ has a dual role as a Brønsted-Lewis acid catalyst for the preparation of biological compounds. For more detail, full characterization of [Zr-UiO-66-PDC-SO_3H]$FeCl_4$ as a catalyst was conducted by FT-IR, VSM, EDX, FE-SEM, elemental mapping, SEM and TEM techniques.

Synthesis and characterization of [Zr-UiO-66-PDC-SO_3H]$FeCl_4$ as a new metal–organic framework (MOF)

The FT-IR analysis of $ZrCl_4$, [Zr-UiO-66-PDC], [Zr-UiO-66-PDC-SO_3H]Cl and [Zr-UiO-66-PDC-SO_3H]$FeCl_4$ is shown in Fig. 4. The broad peak at 2700–3500 cm^{-1} is related to the OH of SO_3H functional group. The aromatic C–H and C=C stretching bands are respectively at 2924 and 1626 cm^{-1}. The absorption bands at 1042 and 1136 cm^{-1} are related to N–S and O–S bond stretching. Furthermore, the absorption bands at 587 cm^{-1} are linked to the stretching vibrational modes of Fe–Cl groups in $FeCl_4$. The FT-IR spectrum difference between starting materials and [Zr-UiO-66-PDC-SO_3H]$FeCl_4$ verified the structure of the catalyst.

The materials in the structure of [Zr-UiO-66-PDC-SO_3H]$FeCl_4$ were characterized by energy dispersive X-ray spectroscopy (EDX) (Fig. 5). The [Zr-UiO-66-PDC-SO_3H]$FeCl_4$ confirmed the existence of Zr, C, O, S, Cl, N and Fe atoms. Furthermore, [Zr-UiO-66-PDC-SO_3H]Cl as a well-dispersed material, was determined and verified by SEM-elemental mapping (Fig. 5).

Also, SEM images of [Zr-UiO-66-PDC-SO_3H]$FeCl_4$ were recorded to investigate the morphology (Fig. 6). The obtained images show the face centred cubic (fcu) structure. In addition, the topography of [Zr-UiO-66-PDC-SO_3H]$FeCl_4$ was studied more closely using transmission electron microscopy (TEM) as shown in Fig. 7. We can see that [Zr-UiO-66-PDC-SO_3H]$FeCl_4$ is a fcu topological network with 12-connected Zr clusters.

After the preparation of [Zr-UiO-66-PDC-SO_3H]$FeCl_4$ *via* the anion exchange method, it was tested as a catalyst for the

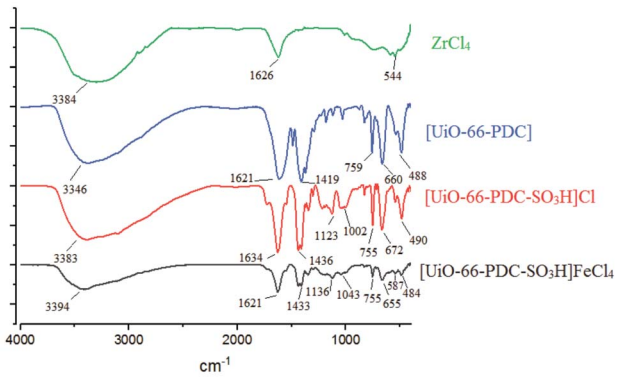

Fig. 4 FT-IR spectra of $ZrCl_4$, [Zr-UiO-66-PDC], [Zr-UiO-66-PDC-SO_3H]Cl and [Zr-UiO-66-PDC-SO_3H]$FeCl_4$.

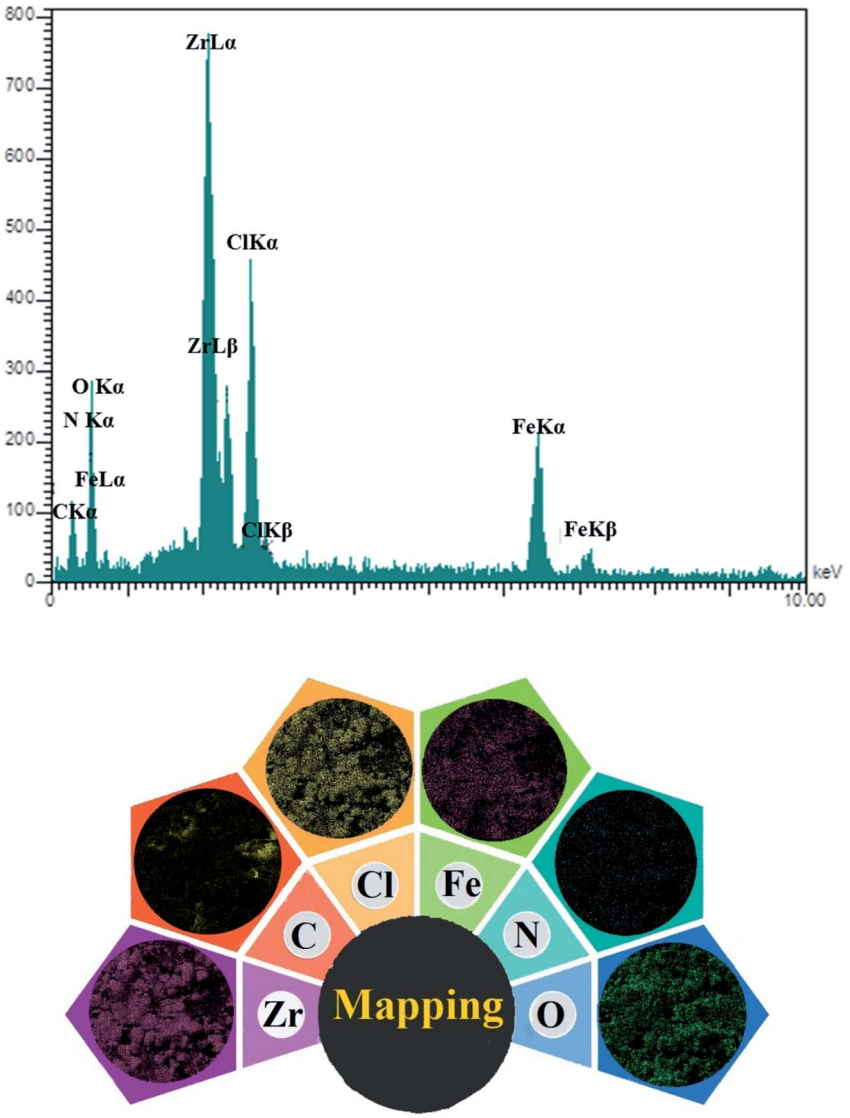

Fig. 5 Upper: energy dispersive X-ray spectroscopy (EDX) of [Zr-UiO-66-PDC-SO_3H]$FeCl_4$. Lower: elemental mapping analysis of [Zr-UiO-66-PDC-SO_3H]$FeCl_4$.

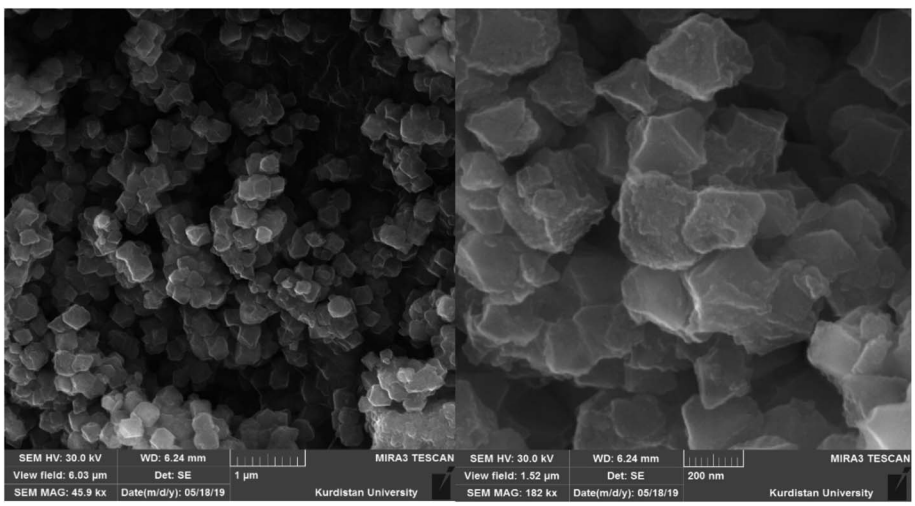

Fig. 6 FE-SEM images of [Zr-UiO-66-PDC-SO_3H]$FeCl_4$.

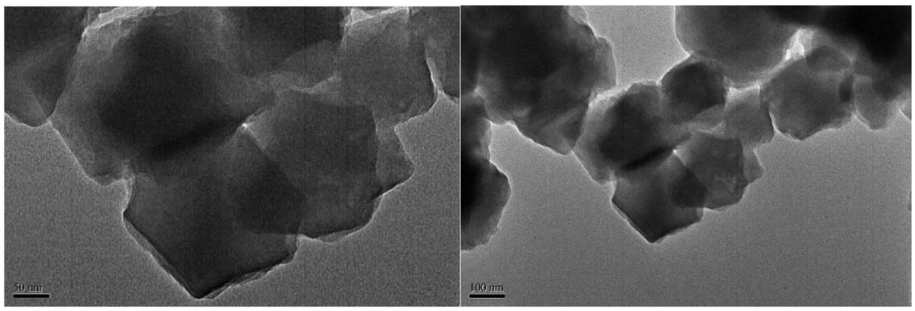

Fig. 7 TEM of [Zr-UiO-66-PDC-SO_3H]$FeCl_4$.

synthesis of new dihydrobenzo[*g*]pyrimido[4,5-*b*]quinoline derivatives with uracil and henna (2-hydroxynaphthalene-1,4-dione) moieties. The above-mentioned products were obtained by reaction of 4-methoxy benzaldehyde (1.0 mmol, 0.136 g), 2-hydroxynaphthalen-1,4-dione (1 mmol, 0.174 g), and 6-amino-1,3-dimethylpyrimidine-2,4(1*H*,3*H*)-dione (1 mmol, 0.155 g) as a model for the optimization of the reaction conditions. The optimized data is listed in Table 1. As shown in Table 1, the best choice for the synthesis of 5-(4-methoxyphenyl)-1,3-dimethyl-5,12-dihydrobenzo[*g*]pyrimido [4,5-*b*]quinoline-2,4,6,11(1*H*,3*H*)-tetraone was achieved in the presence of 10 mg [Zr-UiO-66-PDC-SO_3H]$FeCl_4$ under solvent-free conditions (entry 4, Table 1). The model reaction was also studied under different temperatures and several solvents – H_2O, EtOH, DMF, *n*-hexane, EtOAc, CH_3CN (5 mL) – in the presence of 10 mg of [Zr-UiO-66-PDC-SO_3H]$FeCl_4$. As is shown, the results of the reaction did not improve (Table 1, entries 10–15).

After optimizing the reaction conditions, [Zr-UiO-66-PDC-SO_3H]$FeCl_4$ (10 mg) is applied to synthesize a range of novel biological and pharmacological candidate compounds using various aromatic aldehydes such as trephetaldehyde, *iso*-trephetaldehyde, bearing electron-donating and electron-withdrawing groups, 2-hydroxynaphthalen-1,4-dione and 6-amino-1,3-dimethylpyrimidine-2,4(1*H*,3*H*)-dione. As shown in Table 2, the obtained results indicated that [Zr-UiO-66-PDC-SO_3H]$FeCl_4$ is appropriate for the preparation of target molecules in high to excellent yield (70–90%) with relatively short reaction times (70–120 min).

Table 1 Effect of different amounts of catalyst, solvent and different temperatures, on the synthesis of 5-(4-methoxyphenyl)-1,3-dimethyl-5,12-dihydrobenzo[*g*]pyrimido[4,5-*b*]quinoline-2,4,6,11(1*H*,3*H*)-tetraone

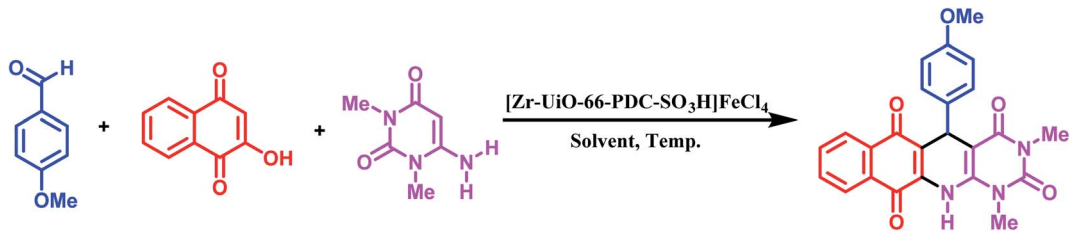

Entry	Amount of catalyst (mg)	Temp. (° C)	Solvent (10 mL)	Time (min)	Yield (%)
1	—	100	—	50	Trace
2	5	100	—	50	45
3	7	100	—	50	50
4	10	100	—	50	90
5	15	100	—	50	90
6	10	r.t.	—	50	75
7	10	50	—	50	70
8	10	70	—	50	20
9	15	120	—	50	90
10	10	Reflux	H_2O	50	85
11	10	Reflux	EtOH	50	70
12	10	100	DMF	50	40
13	10	Reflux	*n*-Hexane	50	Trace
14	10	Reflux	EtOAc	50	Trace
15	10	Reflux	CH_3CN	50	45

Table 2 Synthesis of dihydrobenzo[*g*]pyrimido[4,5-*b*]quinoline derivatives using [Zr-UiO-66-PDC-SO_3H]$FeCl_4$

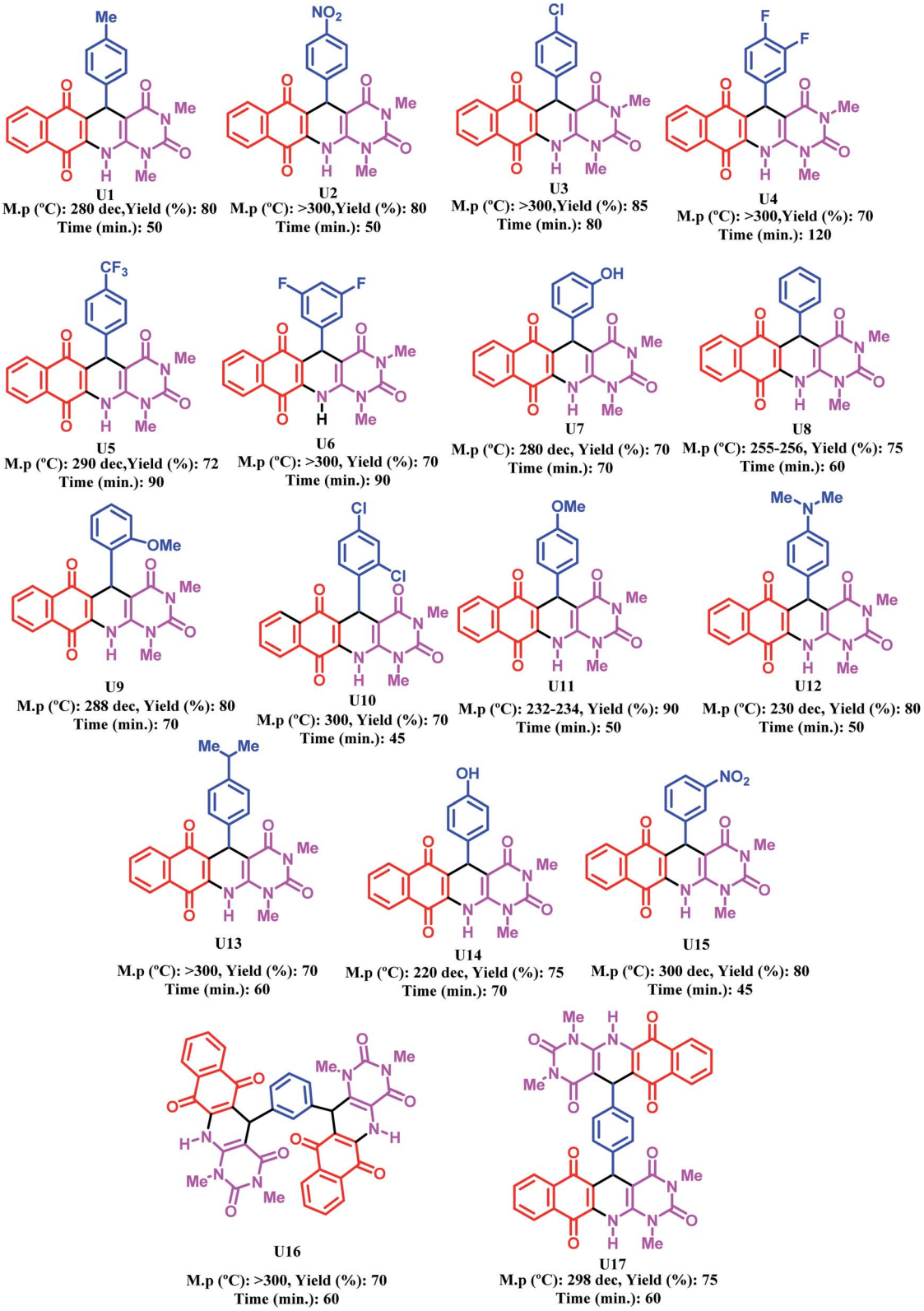

In the proposed mechanism, the [Zr-UiO-66-PDC-SO_3H]$FeCl_4$ catalyst activates the carbonyl functional group of aldehyde. To investigate the activation of the aldehyde, 4-methoxy benzaldehyde was reacted with [Zr-UiO-66-PDC-SO_3H]$FeCl_4$ at room temperature. The FT-IR spectra of the subsequent reaction mixtures were examined.[15,42,43] The absorption bond of

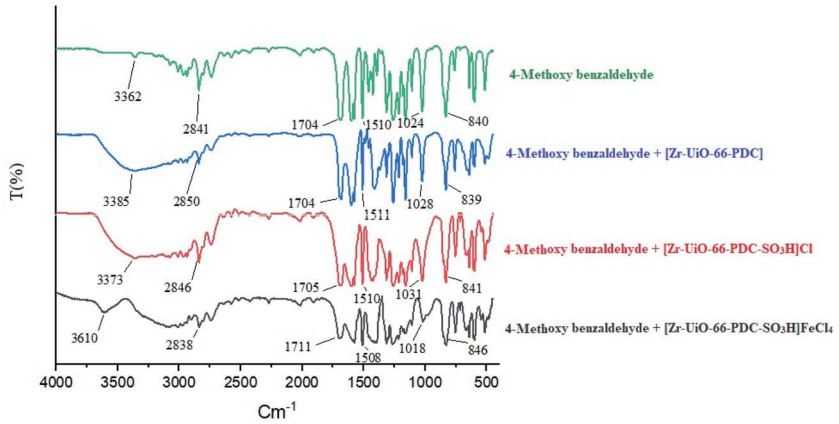

Fig. 8 FT-IR spectra of 4-methoxy benzaldehyde in percent of [Zr-UiO-66-PDC], [Zr-UiO-66-PDC-SO_3H]Cl and [Zr-UiO-66-PDC-SO_3H]$FeCl_4$.

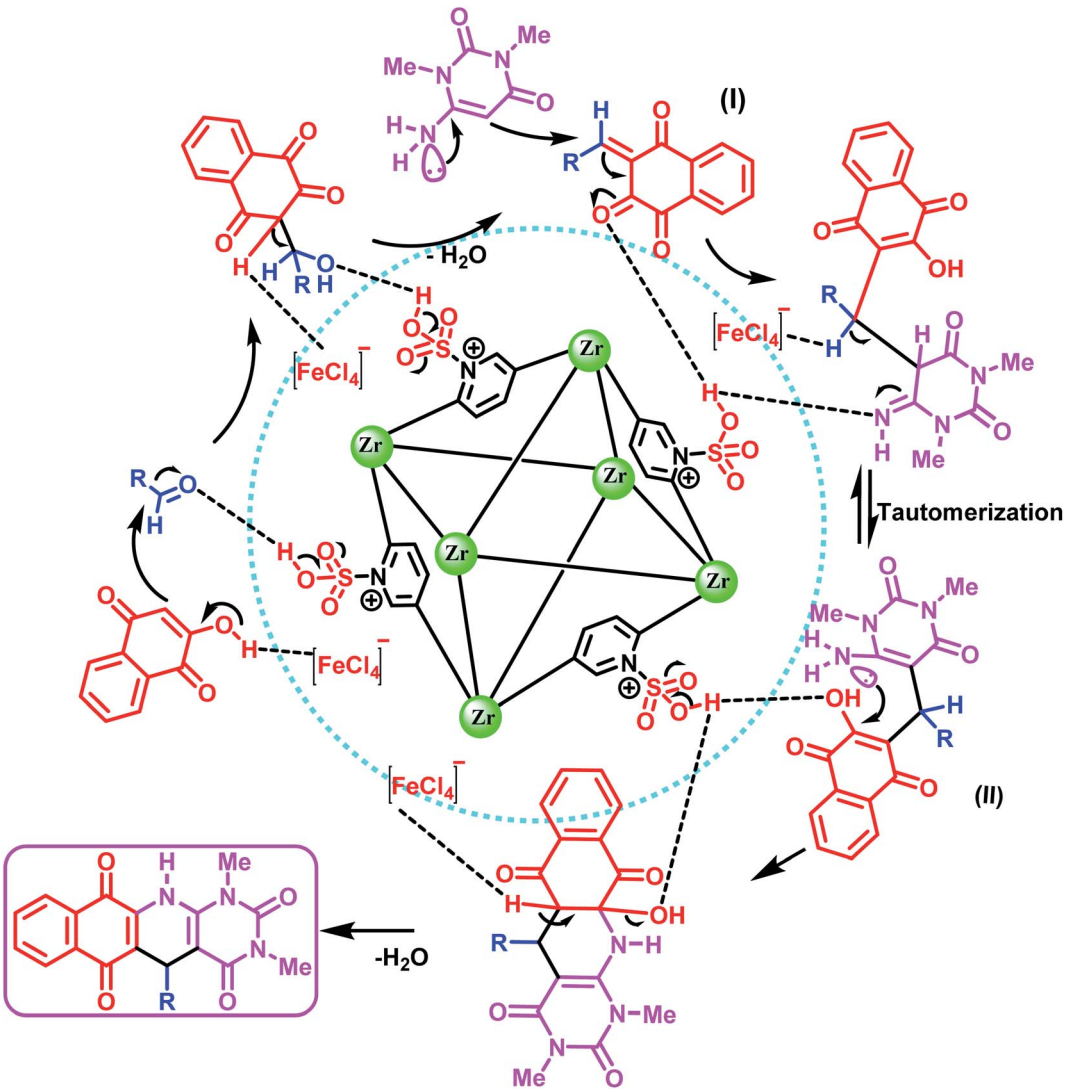

Fig. 9 Proposed mechanism for the synthesis of dihydrobenzo[*g*]pyrimido[4,5-*b*]quinoline derivatives using [Zr-UiO-66-PDC-SO_3H]$FeCl_4$.

C=O of the 4-methoxy benzaldehyde at 1704 cm^{-1}, was changed to 1704, 1705 or 1711 cm^{-1} by [Zr-UiO-66-PDC], [Zr-UiO-66-PDC-SO_3H]Cl and [Zr-UiO-66-PDC-SO_3H]$FeCl_4$ (Fig. 8). Then, the henna (2-hydroxynaphthalen-1,4-dione) moiety reacts with the carbonyl of the aldehyde by removing one H_2O molecule, to give intermediate (I) (Fig. 9). In the next step, 6-amino-1,3-dimethylpyrimidine-2,4(1*H*,3*H*)-dione reacts with intermediate (I) to give intermediate (II). In the next two steps, intermediate (II) gives the desired product after intramolecular cyclization and the loss of another molecule of H_2O.

To evaluate the performance of [Zr-UiO-66-PDC-SO_3H]$FeCl_4$ as a catalyst for the synthesis of dihydrobenzo[*g*]pyrimido[4,5-*b*]quinoline derivatives, we tested various acid catalysts (organic and inorganic) in the reaction of 4-methoxy benzaldehyde (1.0 mmol, 0.136 g), 2-hydroxynaphthalen-1,4-dione (1 mmol, 0.174 g), 6-amino-1,3-dimethylpyrimidine-2,4(1*H*,3*H*)-dione (1 mmol, 0.155 g) as evaluated in Table 3. The obtained results which are collected in Table 3 show that, [Zr-UiO-66-PDC-SO_3H]$FeCl_4$ is the best catalyst for the synthesis of novel dihydrobenzo[*g*]pyrimido[4,5-*b*]quinoline derivatives. The obtained results of catalytic activity and reusability of [Zr-UiO-66-PDC-SO_3H]$FeCl_4$ are shown in Fig. 10. As mentioned above, [Zr-UiO-66-PDC-SO_3H]$FeCl_4$ was separated by centrifugation and reused without significant reduction in its catalytic activity. Recyclability of the catalyst was also studied using the one-pot reaction of 4-methoxy benzaldehyde (1.0 mmol, 0.136 g), 2-hydroxynaphthalen-1,4-dione (1 mmol, 0.174 g), 6-amino-1,3-dimethylpyrimidine-2,4(1*H*,3*H*)-dione (1 mmol, 0.155 g) as a model under the above-mentioned optimized reaction conditions. We found that [Zr-UiO-66-PDC-SO_3H]$FeCl_4$ can be reused up to four times without noticeable changes in its catalytic activity.

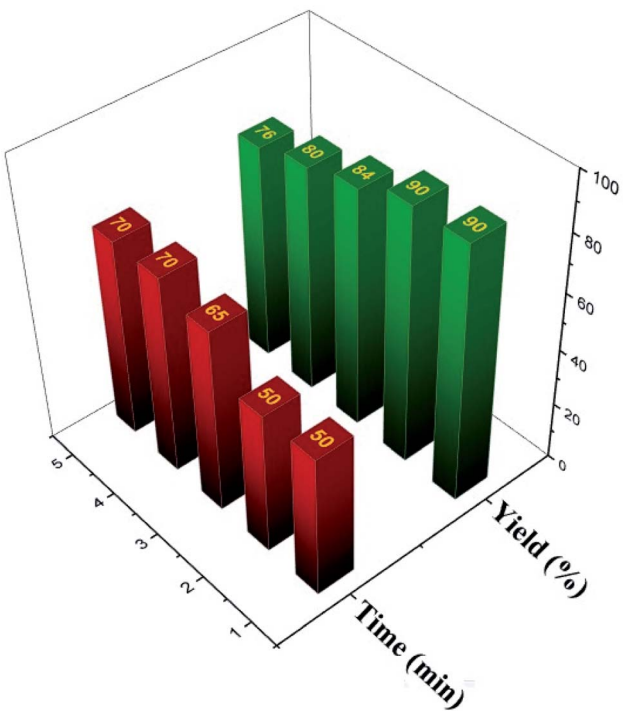

Fig. 10 Recyclability of [Zr-UiO-66-PDC-SO_3H]$FeCl_4$ in the synthesis of dihydrobenzo[*g*]pyrimido[4,5-*b*]quinoline derivatives.

Table 3 Evaluation of various catalysts for the synthesis of 5-(4-methoxyphenyl)-1,3-dimethyl-5,12-dihydrobenzo[*g*]pyrimido[4,5-*b*]quinoline-2,4,6,11(1*H*,3*H*)-tetraone with [Zr-UiO-66-PDC-SO_3H]$FeCl_4$

Entry	Catalyst	Amount of catalyst (mol%)	Time (min)	Yield (%)
1	NaOH	10	60	25
2	Et_3N	10	65	—
3	K_2CO_3	10	70	Trace
4	*P*-TSA	10	90	—
5	SSA [44,45]	10 mg	120	Trace
6	GTBSA [46]	10 mg	80	45
7	[PVI-SO_3H]$FeCl_4$ [19]	10 mg	70	70
8	MIL-100(Cr)–NHEtN$(CH_2PO_3H_2)_2$ [15]	10 mg	60	65
9	Fe_3O_4@Co(BDC-NH_2) [47]	10 mg	50	35
10	CQDs-N$(CH_2PO_3H_2)_2$ [48]	10 mg	80	43
11	TTPA[49]	10	100	55
12	MIL-101(Cr)–N$(CH_2PO_3H_2)_2$ [12]	10 mg	60	80
13	$FeCl_3$	10	120	50
14	$ZrCl_4$	10	120	55
15	Zr-UiO-66-PDC	10 mg	120	40
16	[Zr-UiO-66-PDC-SO_3H]Cl	10 mg	65	75
17	[Zr-UiO-66-PDC-SO_3H]$FeCl_4$	10 mg	50	90

Conclusion

In this study, we have designed, synthesized and introduced [Zr-UiO-66-PDC-SO_3H]$FeCl_4$ as a novel mesoporous catalyst, which was fully characterized using various techniques. To the best of our knowledge, this catalyst is the first MOF that was synthesized *via* the anion exchange method. [Zr-UiO-66-PDC-SO_3H]$FeCl_4$ is an efficient catalyst. It was tested for the preparation of new dihydrobenzo[*g*]pyrimido[4,5-*b*]quinoline derivatives with henna and uracil moieties which have biological interest.

Conflicts of interest

There are no conflicts to declare.

Acknowledgements

We thank Bu-Ali Sina University and the Iran National Science Foundation (INSF) (Grant number: 98001912) for the financial support of our research group.

References

1 H. C. Zhou, J. R. Long and O. M. Yaghi, Introduction to metal–organic frameworks, *Chem. Rev.*, 2012, **112**, 673–674.
2 B. Zornoza, C. Tellez, J. Coronas, J. Gascon and F. Kapteijn, Metal organic framework based mixed matrix membranes: an increasingly important field of research with a large

application potential, *Microporous Mesoporous Mater.*, 2013, **166**, 67–78.
3 R. Ricco, L. Malfatti, M. Takahashi, A. J. Hill and P. Falcaro, Applications of magnetic metal–organic framework composites, *J. Mater. Chem. A*, 2013, **1**, 13033–13045.
4 J. Lee, O. K. Farha, J. Roberts, K. A. Scheidt, S. T. Nguyen and J. T. Hupp, Metal–organic framework materials as catalysts, *Chem. Soc. Rev.*, 2009, **38**, 1450–1459.
5 S. Wang, C. M. McGuirk, A. d'Aquino, J. A. Mason and C. A. Mirkin, Metal–organic framework nanoparticles, *Adv. Mater.*, 2018, **30**, 1800202–1800216.
6 J. Cao, X. Li and H. Tian, Metal–organic framework (MOF)-based drug delivery, *Curr. Med. Chem.*, 2020, **27**, 5949–5969.
7 Y. S. Wei, M. Zhang, R. Zou and Q. Xu, Metal–organic framework-based catalysts with single metal sites, *Chem. Rev.*, 2020, **120**, 12089–12174.
8 S. Chen, Y. Li and L. Mi, Porous carbon derived from metal organic framework for gas storage and separation: the size effect, *Inorg. Chem. Commun.*, 2020, **118**, 107999–108006.
9 H. Sepehrmansourie, Metal Organic Frameworks (MOFs): as multi-purpose catalysts, *Iran. J. Catal.*, 2021, **11**, 207–215.
10 Y. Yang, H. F. Yao, F. G. Xi and E. Q. Gao, *J.* Amino-functionalized Zr (IV) metal–organic framework as bifunctional acid-base catalyst for Knoevenagel condensation, *J. Mol. Catal. A: Chem.*, 2014, **390**, 198–205.
11 J. H. Cavka, S. Jakobsen, U. Olsbye, N. Guillou, C. Lamberti, S. Bordiga and K. P. Lillerud, A new zirconium inorganic building brick forming metal organic frameworks with exceptional stability, *J. Am. Chem. Soc.*, 2008, **130**, 13850–13851.
12 S. Babaee, M. Zarei, H. Sepehrmansourie, M. A. Zolfigol and S. Rostamnia, Synthesis of metal–organic frameworks MIL-101(Cr)-NH_2 containing phosphorous acid functional groups: application for the synthesis of *N*-Amino-2-pyridone and pyrano [2, 3-*c*] pyrazole derivatives *via* a cooperative vinylogous anomeric-based oxidation, *ACS Omega*, 2020, **5**, 6240–6249.
13 S. Babaee, M. Zarei, M. A. Zolfigol, S. Khazalpour, M. Hasani, U. Rinner, R. Schirhagl, N. Norouzi and S. Rostamnia, Synthesis of biological based hennotannic acid-based salts over porous bismuth coordination polymer with phosphorous acid tags, *RSC Adv.*, 2021, **11**, 2141–2157.
14 A. M. Naseri, M. Zarei, S. Alizadeh, S. Babaee, M. A. Zolfigol, D. Nematollahi, J. Arjomandi and H. Shi, Synthesis and application of [Zr-UiO-66-PDC-SO_3H]Cl MOFs to the preparation of dicyanomethylene pyridines *via* chemical and electrochemical methods, *Sci. Rep.*, 2021, **11**, 1–19.
15 H. Sepehrmansouri, M. Zarei, M. A. Zolfigol, A. R. Moosavi-Zare, S. Rostamnia and S. Moradi, Multilinker phosphorous acid anchored En/MIL-100(Cr) as a novel nanoporous catalyst for the synthesis of new *N*-heterocyclic pyrimido [4, 5-*b*] quinolines, *Mol. Catal.*, 2020, **481**, 110303–110320.
16 M. A. Zolfigol, A. Khazaei, A. R. Moosavi-Zare, A. Zare and V. Khakyzadeh, Rapid synthesis of 1-amidoalkyl-2-naphthols over sulfonic acid functionalized imidazolium salts, *Appl. Catal., A*, 2011, **400**, 70–81.
17 S. Babaee, M. A. Zolfigol, M. Zarei, M. Abbasi and Z. Najafi, Synthesis of pyridinium-based salts: catalytic application at the synthesis of six membered *O*-heterocycles, *Mol. Catal.*, 2019, **475**, 110403–110417.
18 M. A. Zolfigol, A. Khazaei, A. R. Moosavi-Zare and A. Zare, Ionic liquid 3-Methyl-1-sulfonic acid imidazolium chloride as a novel and highly efficient catalyst for the very rapid synthesis of bis(indolyl)methanes under solvent-free conditions, *Org. Prep. Proced. Int.*, 2010, **42**, 95–102.
19 H. Sepehrmansourie, M. Zarei, R. Taghavi and M. A. Zolfigol, Mesoporous ionically tagged cross-linked poly(vinyl imidazole)s as novel and reusable catalysts for the preparation of *N*-heterocycle spiropyrans, *ACS Omega*, 2019, **4**, 17379–17392.
20 H. Sepehrmansourie, M. Zarei, M. A. Zolfigol, A. Mehrzad and H. R. Hafizi-Atabak, Application of [PVI-SO_3H]NO_3 as a novel polymeric nitrating agent with ionic tags in preparation of high-energetic materials, *RSC Adv.*, 2021, **11**, 8367–8374.
21 M. Zarei, E. Noroozizadeh, A. R. Moosavi-Zare and M. A. Zolfigol, Synthesis of nitroolefins and nitroarenes under mild conditions, *J. Org. Chem.*, 2018, **83**, 3645–3650.
22 W. Zhu, Y. Pei, Y. Liu, J. Zhang, Y. Qin, Y. Yin and M. D. Guiver, Mass transfer in a Co/N/C catalyst layer for the anion exchange membrane fuel cell, *ACS Appl. Mater. Interfaces*, 2020, **12**, 32842–32850.
23 M. A. Zolfigol, A. Khazaei, A. R. Moosavi-Zare, A. Zare, H. G. Kruger, Z. Asgari, V. Khakyzadeh and M. Kazem-Rostami, Design of ionic liquid 3-methyl-1-sulfonic acid imidazolium nitrate as reagent for the nitration of aromatic compounds by *in situ* generation of NO_2 in acidic Media, *J. Org. Chem.*, 2012, **77**, 3640–3645.
24 H. Sepehrmansourie, Magnetic ionic liquids: as multi-purpose catalysts, *Iran. J. Catal.*, 2020, **10**, 337–341.
25 H. R. Hudson, N. J. Wardle, S. WA Bligh, I. Greiner, A. Grun and G. Keglevich, *N*-heterocyclic dronic acids: applications and synthesis, *Mini-Rev. Med. Chem.*, 2012, **12**, 313–325.
26 M. De Luca, G. Ioele and G. Ragno, 1, 4-dihydropyridine antihypertensive drugs: Recent advances in photostabilization strategies, *Pharmaceutics*, 2019, **11**, 85–98.
27 G. Ragno, C. Vetuschi, A. Risoli and G. Ioele, Application of a classical least-squares regression method to the assay of 1, 4-dihydropyridine antihypertensives and their photoproducts, *Talanta*, 2003, **59**, 375–382.
28 S. Moradi, M. A. Zolfigol, M. Zarei, D. A. Alonso and A. Khoshnood, An efficient catalytic method for the synthesis of pyrido[2,3-*d*]pyrimidines as biologically drug candidates by using novel magnetic nanoparticles as a reusable catalyst, *Appl. Organomet. Chem.*, 2018, **32**, 4043–4061.
29 F. Jalili, M. Zarei, M. A. Zolfigol, S. Rostamnia and A. R. Moosavi-Zare, SBA-15/PrN$(CH_2PO_3H_2)_2$ as a novel and efficient mesoporous solid acid catalyst with phosphorous acid tags and its application on the synthesis of new pyrimido[4,5-*b*]quinolones and pyrido[2,3-*d*]pyrimidines *via*

anomeric based oxidation, *Microporous Mesoporous Mater.*, 2020, **294**, 109865.

30 W. Yu and C. Li, Regioselective one-pot C–N coupling of substituted naphthoquinones: selective intramolecular ring fusion of sulfonamides, *Tetrahedron*, 2014, **70**, 459–464.

31 J. Tyleckova, R. Hrabakova, K. Mairychova, P. Halada, L. Radova, P. Dzubak, M. Hajduch, S. J. Gadher and H. Kovarova, Cancer cell response to anthracyclines effects: mysteries of the hidden proteins associated with these drugs, *Int. J. Mol. Sci.*, 2012, **13**, 15536–15564.

32 S. ElKalyoubi and E. Fayed, Synthesis and evaluation of antitumour activities of novel fused tri-and tetracyclic uracil derivatives, *J. Chem. Res.*, 2016, **40**, 771–777.

33 I. Nizhenkovska, Standardization of citrullus colocynthis (L.) Shrad. fruitsdry extract for futher study of its antidiabetic activity, *Am. J. Clin. Exp. Immunol.*, 2015, **3**, 162.

34 T. Mirsaev, Experimental study of hepatoprotective activity of hydroxymethyluracil, *Bull. Exp. Biol. Med.*, 2007, **143**, 575–576.

35 M. Eltze, Investigations on the mode of action of a new antihypertensive drug, urapidil, in the isolated rat vas deferens, *Eur. J. Pharmacol.*, 1979, **59**, 1–9.

36 J. I. Bardagi and R. A. Rossi, Advances in the synthesis of 5- and 6-substituted uracil derivatives, *Org. Prep. Proced. Int.*, 2009, **41**, 479–514.

37 A. Mai, D. Rotili, S. Massa, G. Brosch, G. Simonetti, C. Passariello and A. T. Palamara, Discovery of uracil-based histone deacetylase inhibitors able to reduce acquired antifungal resistance and trailing growth in candida albicans, *Bioorg. Med. Chem. Lett.*, 2007, **17**, 1221–1225.

38 T. Tomašić and L. Peterlin Mašič, Rhodanine as a scaffold in drug discovery: a critical review of its biological activities and mechanisms of target modulation, *Expert Opin. Drug Discovery*, 2012, **7**, 549–560.

39 I. Yousefi, M. Pakravan, H. Rahimi, A. Bahador, Z. Farshadzadeh and I. Haririan, An investigation of electro spun Henna leaves extract-loaded chitosan based nanofibrous mats for skin tissue engineering, *Mater. Sci. Eng., C*, 2017, **75**, 433–444.

40 (*a*) M. A. Zolfigol, A. Khazaei, S. Alaie and S. Baghery, Synthesis of tricyanomethanesulfonic acid as a novel nanostructured and recyclable solid acid: application at the synthesis of biological henna-based chromenes, *Can. J. Chem.*, 2017, **95**, 560–570; (*b*) M. Zarei, M. A. Zolfigol, A. R. Moosavi-Zare and E. Noroozizadeh, Trityl bromide *versus* nano-magnetic catalyst in the synthesis of henna-based xanthenes and bis-coumarins, *J. Iran. Chem. Soc.*, 2017, **14**, 2187–2198; (*c*) M. Yarie, M. A. Zolfigol, S. Babaee, S. Baghery, D. A. Alonso and A. Khoshnood, Catalytic application of a nano-molten salt catalyst in the synthesis of biological naphthoquinone-based compounds, *Res. Chem. Intermed.*, 2018, **44**, 2839–2852; (*d*) S. Moradi, M. A. Zolfigol, M. Zarei, D. A. Alonso and A. Khoshnood, Synthesis of a biological-based glycoluril with phosphorous acid tags as a new nanostructured catalyst: application for the synthesis of novel natural Henna-based compounds, *ChemistrySelect*, 2018, **3**, 3042; (*e*) M. Dashteh, S. Baghery, M. A. Zolfigol, A. Khazaei, S. Makhdoomi, M. Safaiee, J. Rakhtshah, Y. Bayat and A. Asgari, Design and synthesis of nickel tetra-2,3-pyridiniumporphyrazinato trinitromethanide as an influential catalyst and its application in the synthesis of 1,2,4-triazolo based compounds, *J. Phys. Chem. Solids*, 2022, **160**, 110322; (*f*) M. Dashteh, M. Safaiee, S. Baghery and M. A. Zolfigol, Application of cobalt phthalocyanine as a nanostructured catalyst in the synthesis of biological henna-based compounds, *Appl. Organomet. Chem.*, 2019, **33**, e4690.

41 S. Waitschat, D. Fröhlich, H. Reinsch, H. Terraschke, K. Lomachenko, C. Lamberti, H. Kummer, T. Helling, M. Baumgartner and S. Henninger, Synthesis of M-UiO-66 (M= Zr, Ce or Hf) employing 2,5-pyridinedicarboxylic acid as a linker: defect chemistry, framework hydrophilization and sorption properties, *Dalton Trans.*, 2018, **47**, 1062–1070.

42 S. Babaee, M. A. Zolfigol, M. Zarei and J. Zamanian, 1,10-Phenanthroline-Based Molten Salt as a Bifunctional Sulfonic Acid Catalyst: Application to the Synthesis of *N*-Heterocycle Compounds *via* Anomeric Based Oxidation, *ChemistrySelect*, 2018, **3**, 8947–8954.

43 S. E. John, S. Gulati and N. Shankaraiah, Recent advances in multi-component reactions and their mechanistic insights: A triennium review, *Org. Chem. Front.*, 2021, **8**, 4237–4287.

44 M. A. Zolfigol, Silica sulfuric acid/$NaNO_2$ as a novel heterogeneous system for production of thionitrites and disulfides under mild conditions, *Tetrahedron*, 2001, **57**, 9509–9511.

45 H. Sepehrmansourie, Silica sulfuric acid (SSA): as a multipurpose catalyst, *Iran. J. Catal.*, 2020, **10**, 175–179.

46 M. Zarei, H. Sepehrmansourie, M. A. Zolfigol, R. Karamian and S. H. M. Farida, Novel nano-size and crab-like biological-based glycoluril with sulfonic acid tags as a reusable catalyst: its application to the synthesis of new mono-and bis-spiropyrans and their *in vitro* biological studies, *New J. Chem.*, 2018, **42**, 14308–14317.

47 H. Sepehrmansourie, M. Zarei, M. A. Zolfigol, S. Babaee and S. Rostamnia, Application of novel nanomagnetic metal–organic frameworks as a catalyst for the synthesis of new pyridines and 1,4-dihydropyridines *via* a cooperative vinylogous anomeric based oxidation, *Sci. Rep.*, 2021, **11**, 1–15.

48 M. M. Rasooll, M. Zarei, M. A. Zolfigol, H. Sepehrmansourie, A. Omidi, M. Hasani and Y. Gu, Novel nano-architectured carbon quantum dots (CQDs) with phosphorous acid tags as an efficient catalyst for the synthesis of multisubstituted 4*H*-pyran with indole moieties under mild conditions, *RSC Adv.*, 2021, **11**, 25995–26007.

49 S. Kalhor, M. Zarei, H. Sepehrmansourie, M. A. Zolfigol, H. Shi, J. Wang, J. Arjomandi, M. Hasani and R. Schirhagl, Novel uric acid-based nano organocatalyst with phosphorous acid tags: application for synthesis of new biologically-interest pyridines with indole moieties *via* a cooperative vinylogous anomeric based oxidation, *Mol. Catal.*, 2021, **507**, 111549.